Supporting Information

Structural Insights and Electronic State Analysis of PtNi Nanowire Catalysts by *operando* High-Energy Resolution Fluorescence Detection X-ray Absorption Spectroscopy

Weijie Cao, [a] *Neha Thakur,* [*a] *Mukesh Kumar,* [a] *Tomoki Uchiyama,* [a] *Yunfei Gao,* [a] *Satoshi Tominaka,* [b] *Akihiko Machida,* [c] *Toshiki Watanabe,* [a] *Ryota Sato,* [d] *Toshiharu Teranishi,* [d] *Masashi Matsumoto,*[e] *Hideto Imai,* [e] *Yoshiharu Sakurai,* [f] *Yoshiharu Uchimoto* [a]

[a] Graduate School of Human and Environmental Studies, Kyoto University, Yoshida Nihonmatsu-cho, Sakyo-ku, Kyoto 606-8501, Japan

[b] International Centre for Materials Nanoarchitectonics (MANA), National Institute for Materials Science (NIMS), 1-1 Namiki, Tsukuba, Ibaraki 305-0044, Japan

[c] Synchrotron Radiation Research Center, National Institutes for Quantum and Radiological Science and Technology, 1-1-1, Kouto, Sayo-cho, Sayo-gun, Hyogo 679-5148, Japan

[d] Institute for Chemical Research, Kyoto University, Uji, Kyoto 611-0011, Japan

[e] Fuel Cell Cutting-Edge Research Center Technology Research Association, Aomi, Koto, Tokyo, 135-0064 Japan

[f] Japan Synchrotron Radiation Research Institute (JASRI), Koto, Sayo, Hyogo, 679-5198, Japan

[*]*Corresponding author: thakur.neha.2x@kyoto-u.ac.jp*

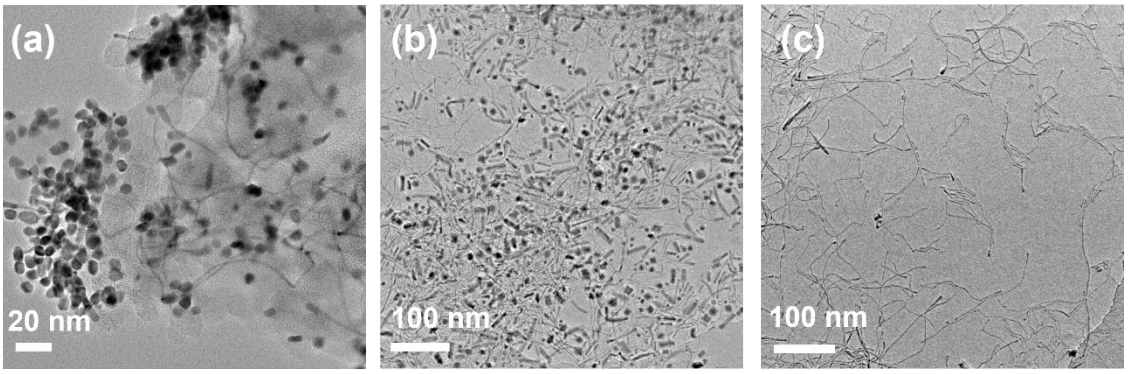

Fig. S1. TEM image of Pt-NW catalyst synthesized using (a) 0 mg, (b) 2.5 mg and (c) 6.4 mg $Ni(acac)_2$.

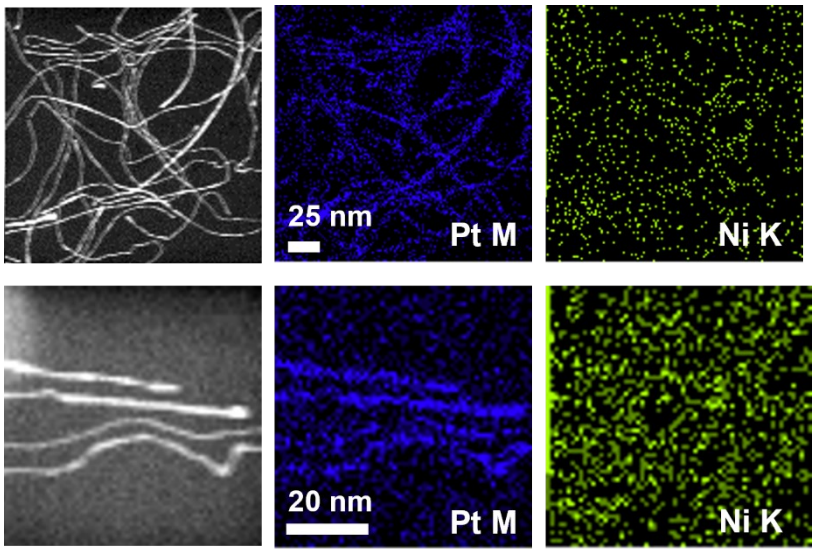

Fig. S2. STEM-EDS element mapping spectrum of Pt-NW/C.

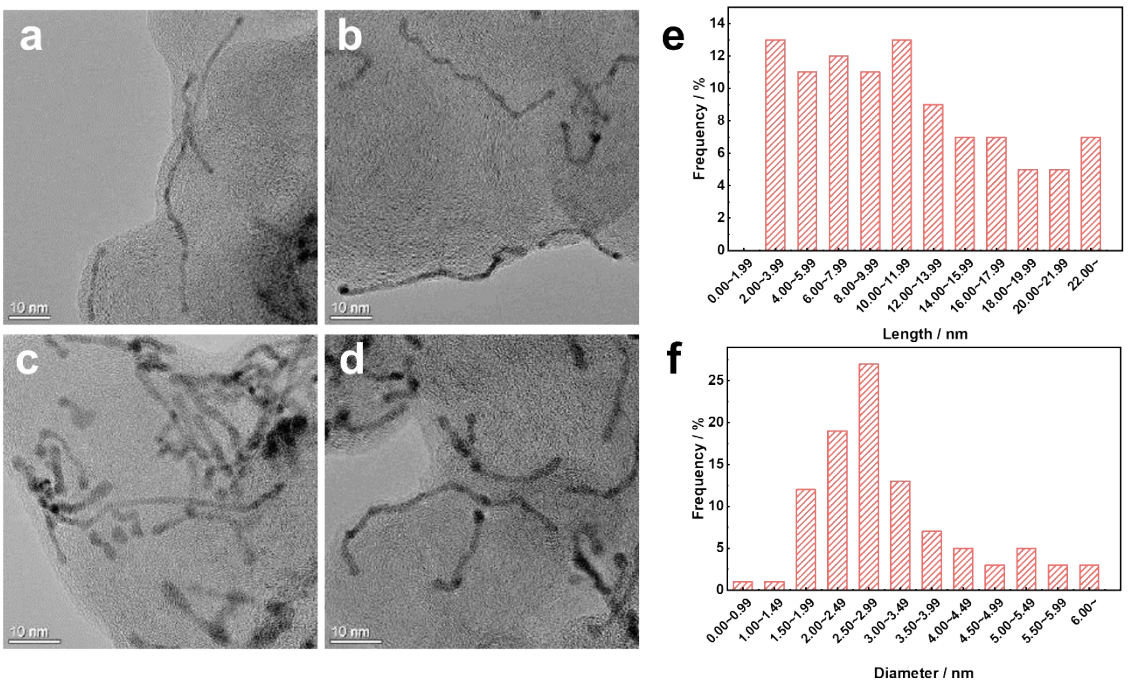

Fig. S3. (a-d) TEM images, (e) length distribution and (f) diameter distribution of Pt-NW/C.

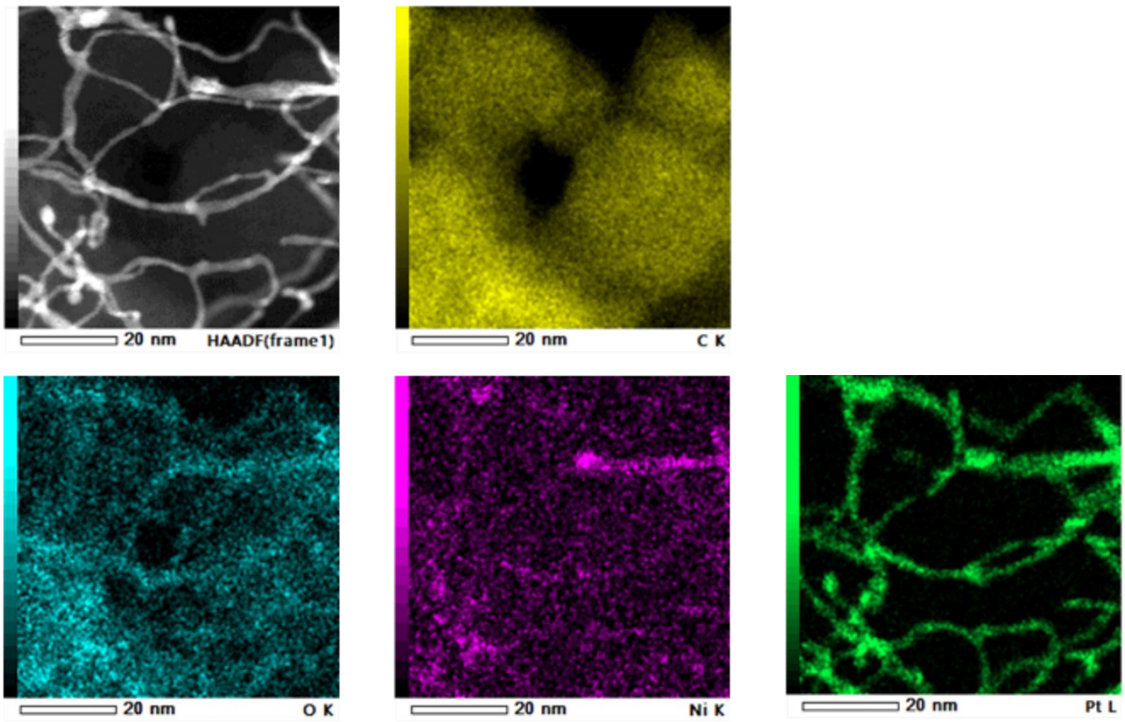

Fig. S4. STEM image and EDS element mapping for PtNi-NW/C before H_2/N_2 annealing treatment.

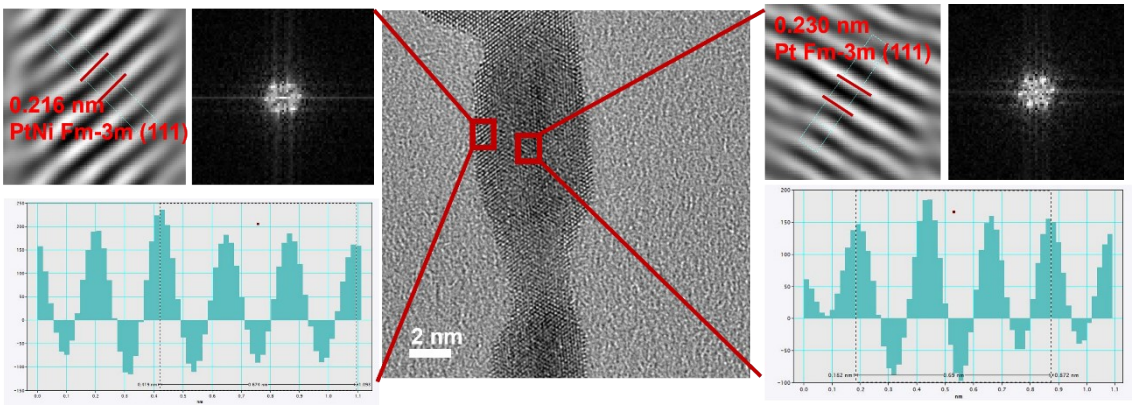

Fig. S5. HRTEM and FFT patterns of PtNi-NW/C without annealing treatment.

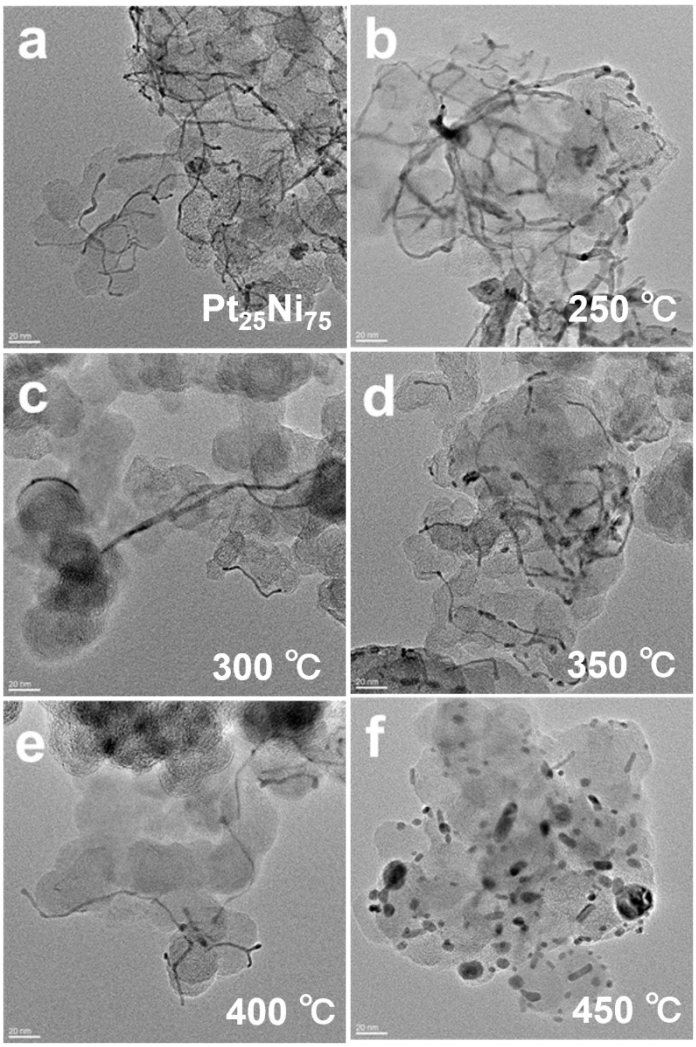

Fig. S6. TEM image of PtNi-NW/C (a) before and after (b) 250 ℃, (c) 300 ℃, (d) 350 ℃, (e) 400 ℃ and (f) 450 ℃ H_2/N_2 annealing treatment.

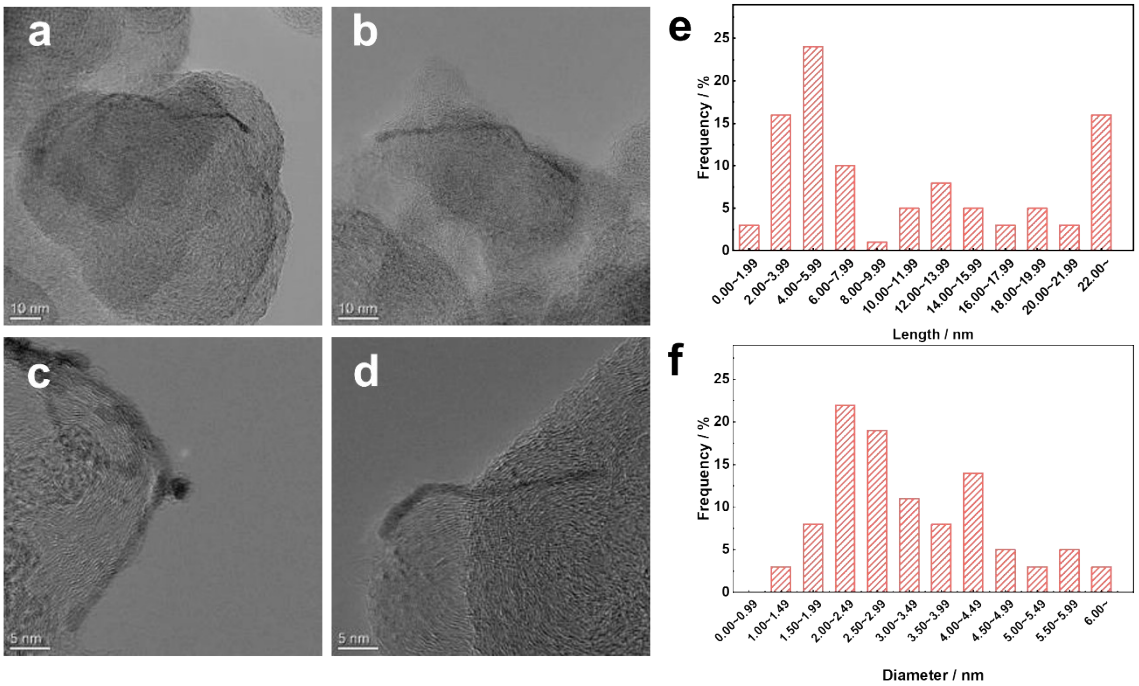

Fig. S7. (a-d) TEM images, (e) length distribution and (f) diameter distribution of PtNi-NW/C.

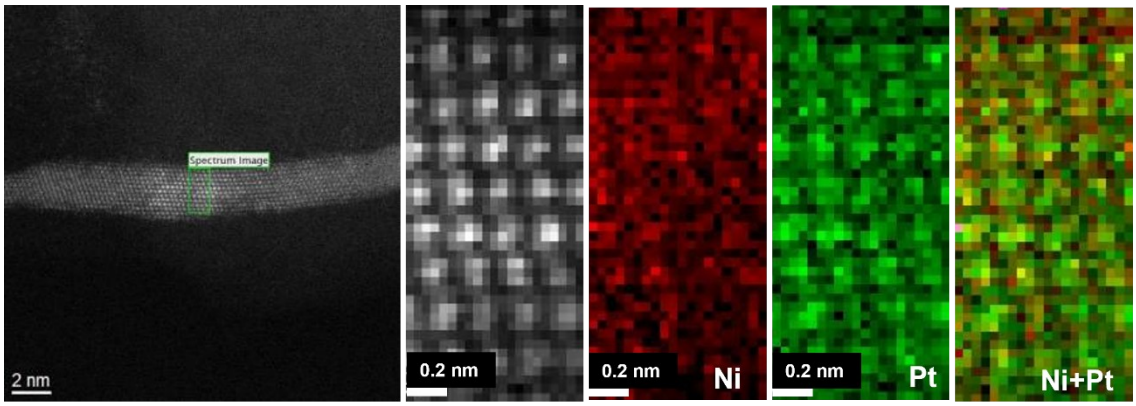

Fig. S8. STEM-EELS mappings for PtNi-NW/C after 300°C annealing treatment.

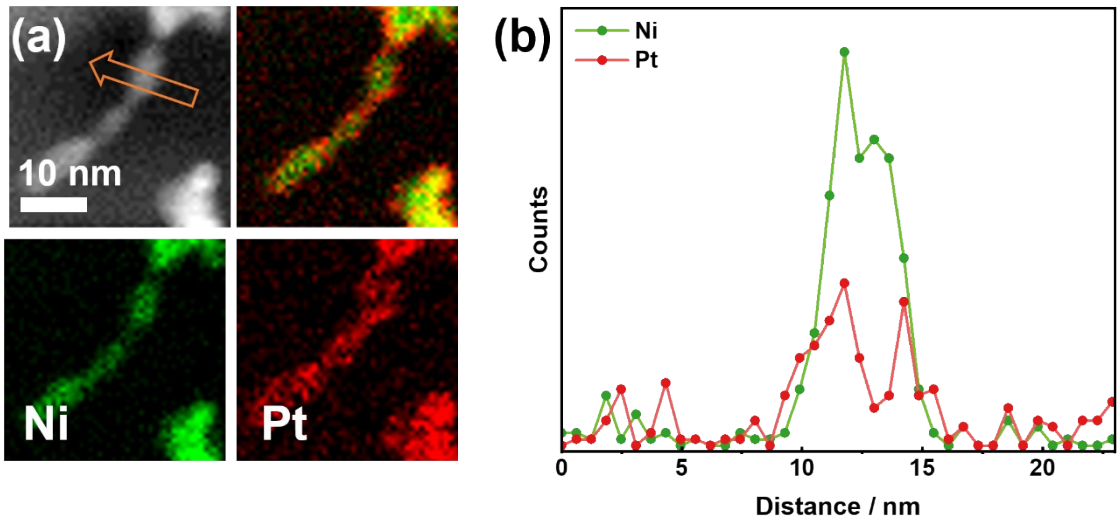

Fig. S9. (a) STEM-EDS element mapping spectrum, and (b) line scanning profiles of PtNi-NW/C.

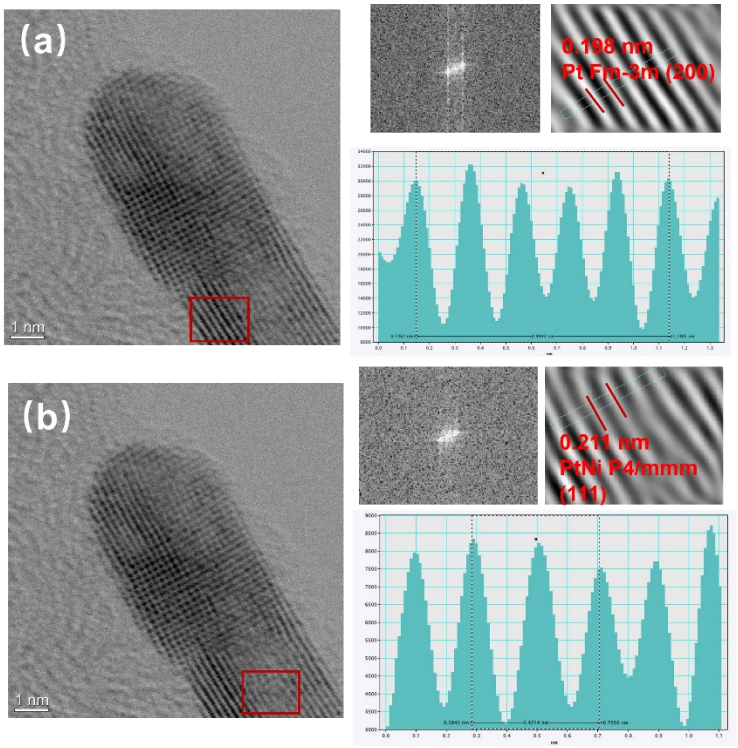

Fig. S10. HRTEM and FFT patterns of PtNi-NW/C in (a) Pt-rich layer and (b) PtNi alloy core.

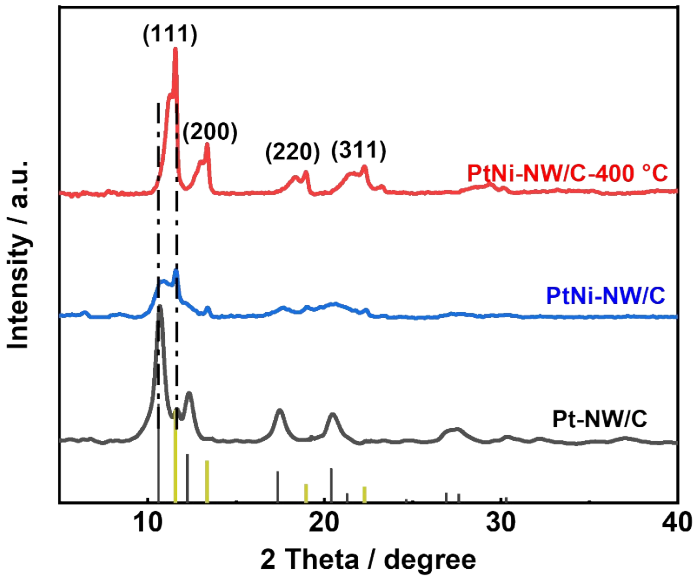

Fig. S11. XRD pattern for Pt-NW/C, PtNi-NW/C before and after 400℃ annealing treatments. The yellow bar is standard Ni and the gray bar is standard Pt.

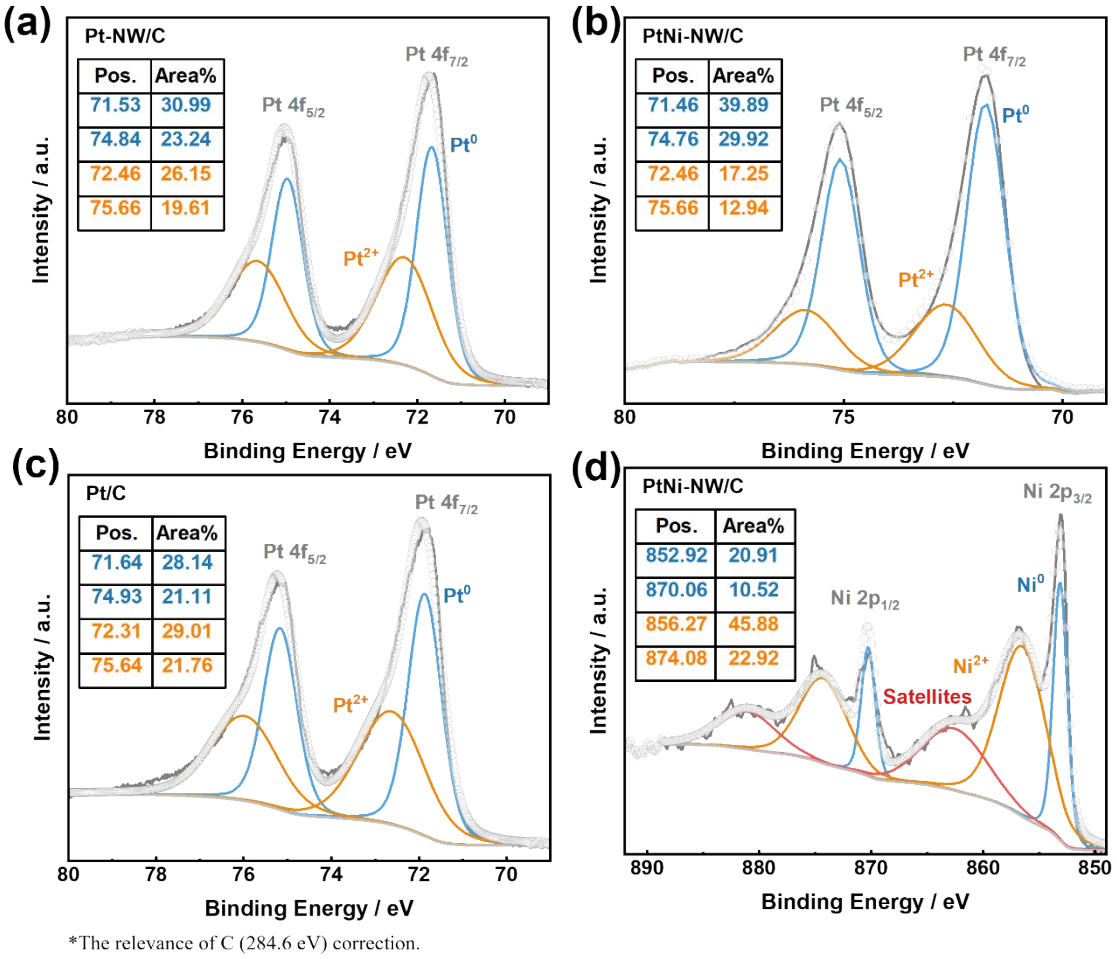

*The relevance of C (284.6 eV) correction.

Fig. S12. XPS spectra for the (a) Pt-NW/C, (b) PtNi-NW/C and (c) Pt/C of Pt 4f and (d) Ni 2p.

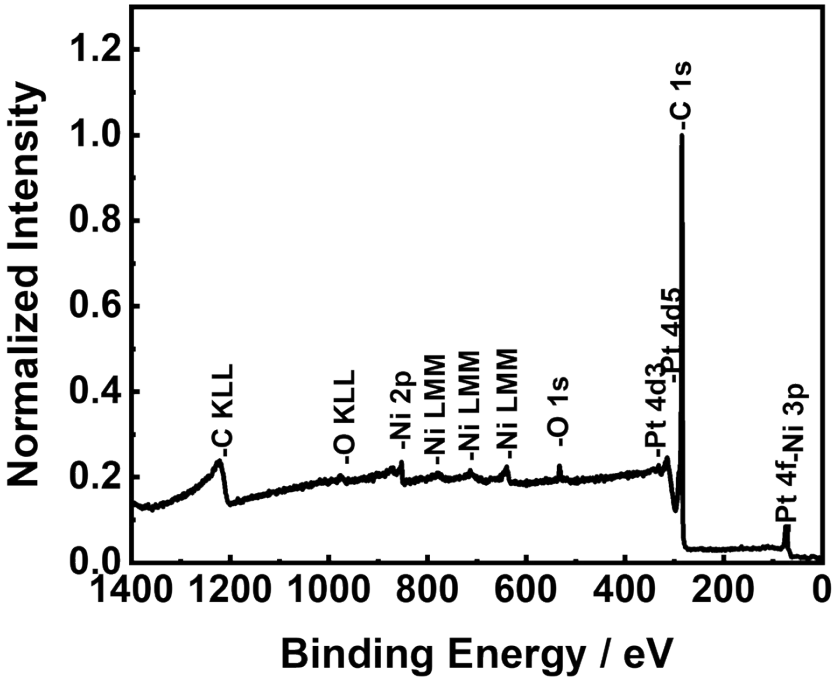

Fig. S13. XPS survey spectra of PtNi-NW/C.

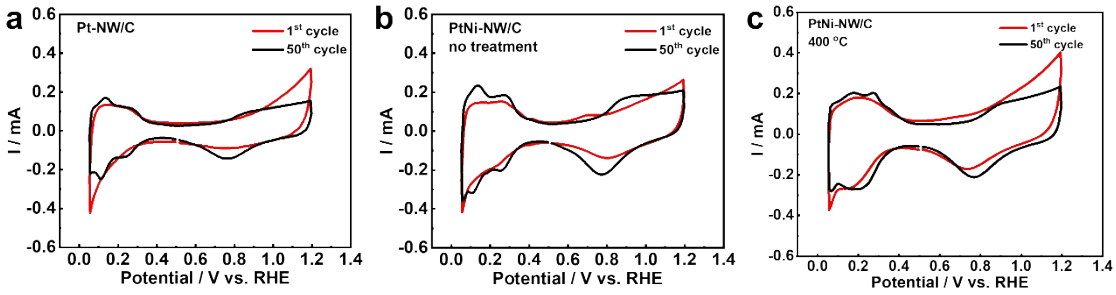

Fig. S14. CV curves of (a) Pt-NW/C, (b) PtNi-NW/C before annealing and (c) PtNi-NW/C after 400 ℃ treatment at a scanning rate for 100 mV/s.

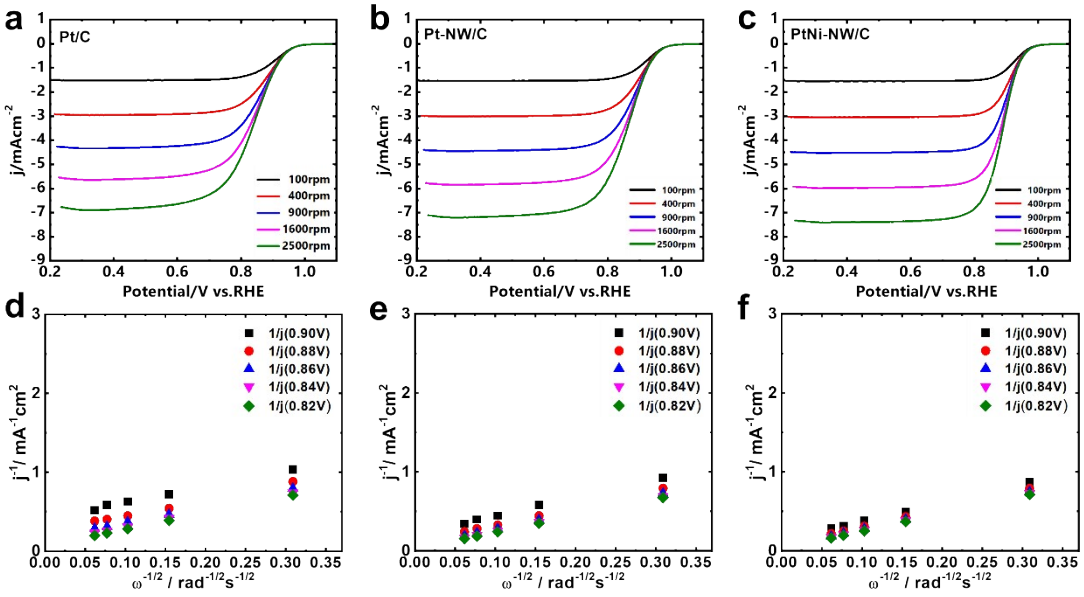

Fig. S15. LSV curves and Koutecky-Levich plots for (a, d) Pt/C, (b, e) Pt-NW/C, and (c, f) PtNi-NW/C in O_2-saturated 0.1 M $HClO_4$ solution at different rotating speed.

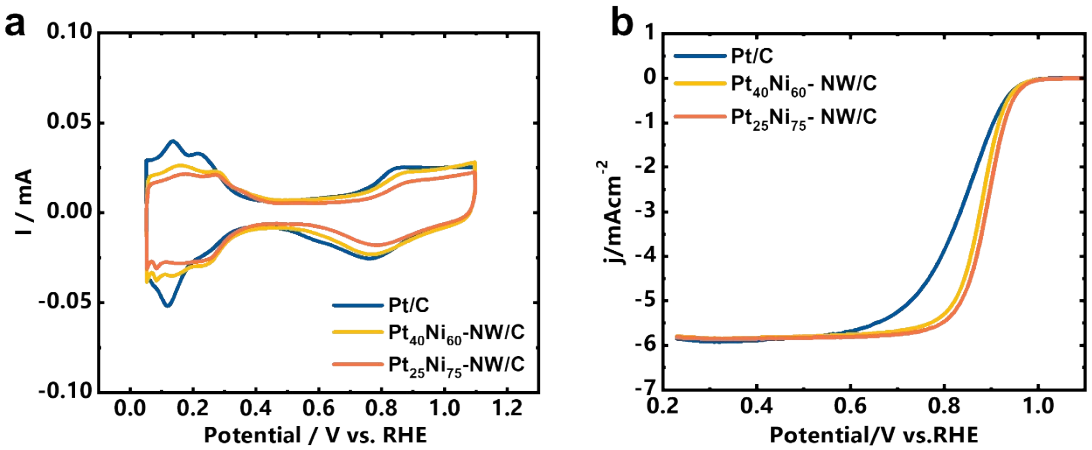

Fig. S16. (a) CV and (b) LSV curves of PtNi-NW/C catalyst with different Ni content.

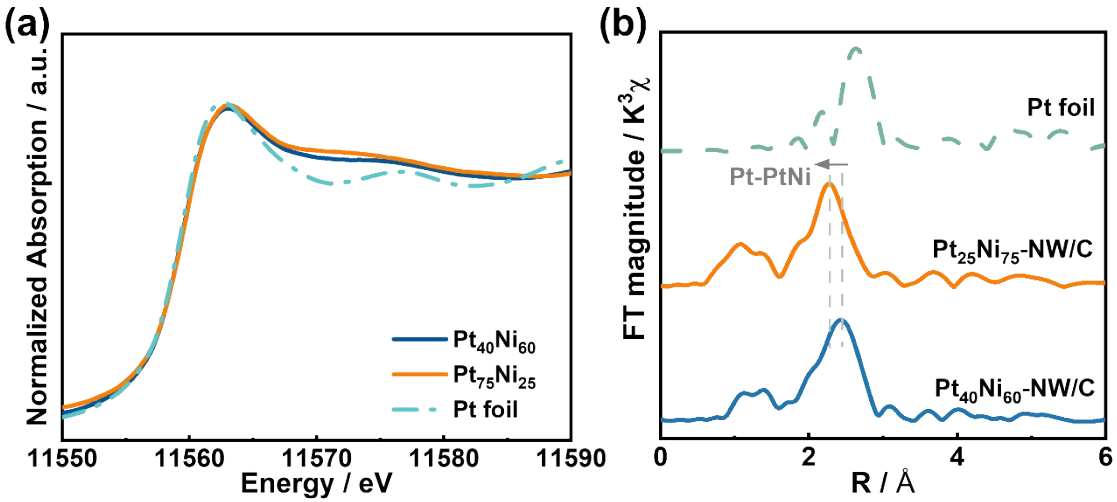

Fig. S17. (a) Pt L_3-edge XANES spectra and (b) FT-EXAFS spectra of PtNi-NW/C with different Ni content.

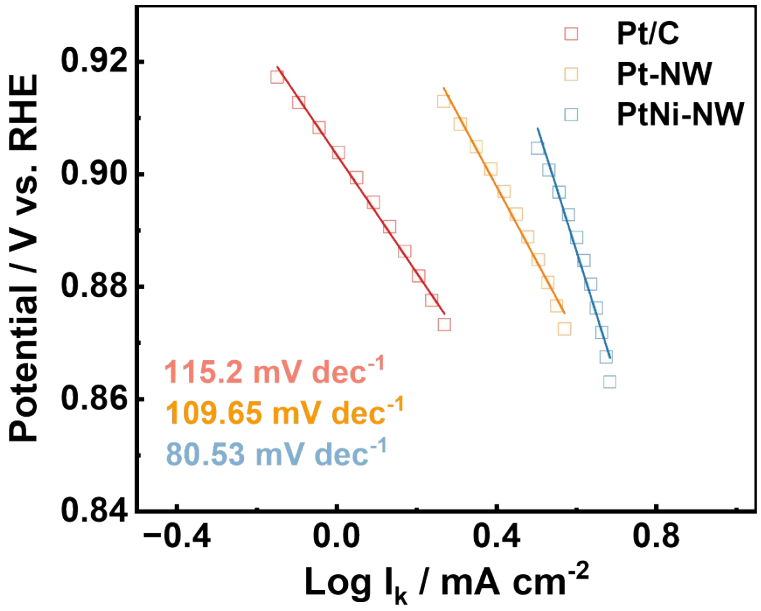

Fig. S18. Tafel plots of specific activity.

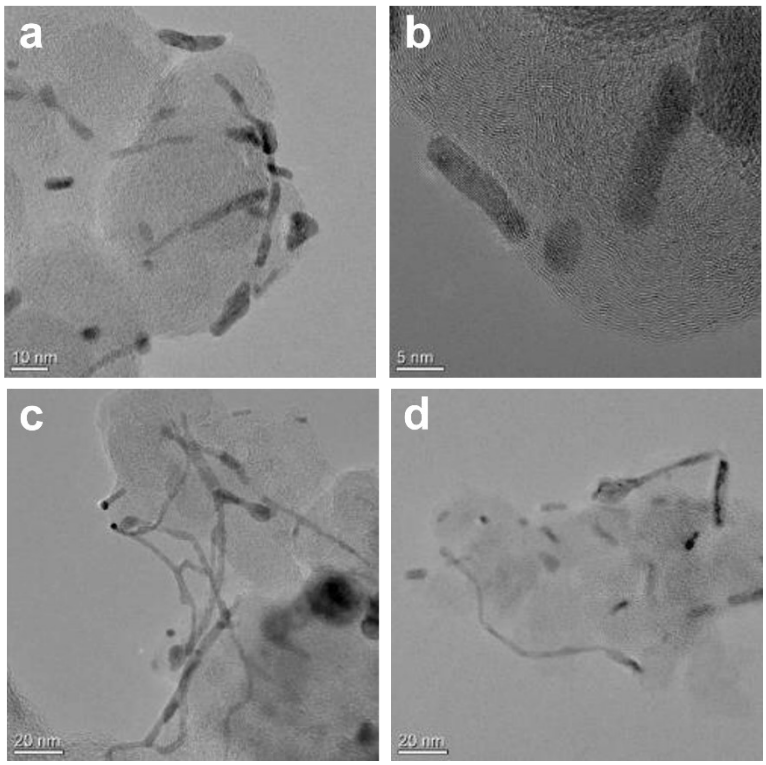

Fig. S19. TEM images of (a,b) Pt-NW/C and (c,d) PtNi-NW/C catalyst after 10K ADT cycles.

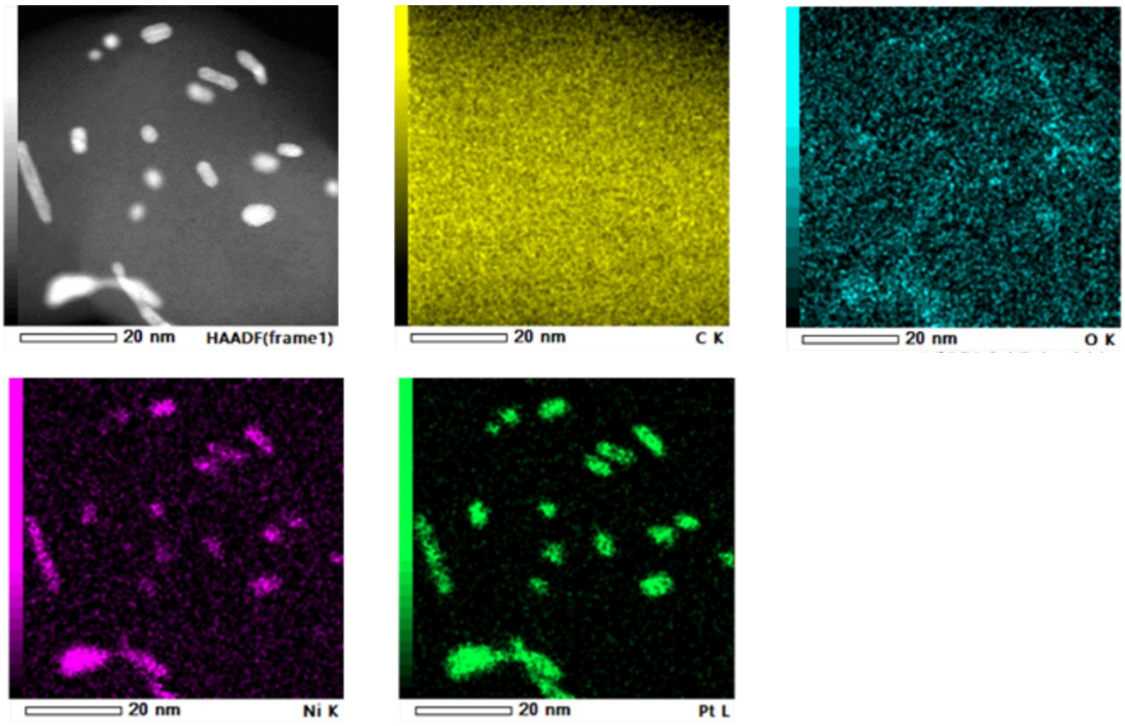

Fig. S20. STEM image and EDS element mapping for PtNi-NW/C catalyst after 10K ADT cycles.

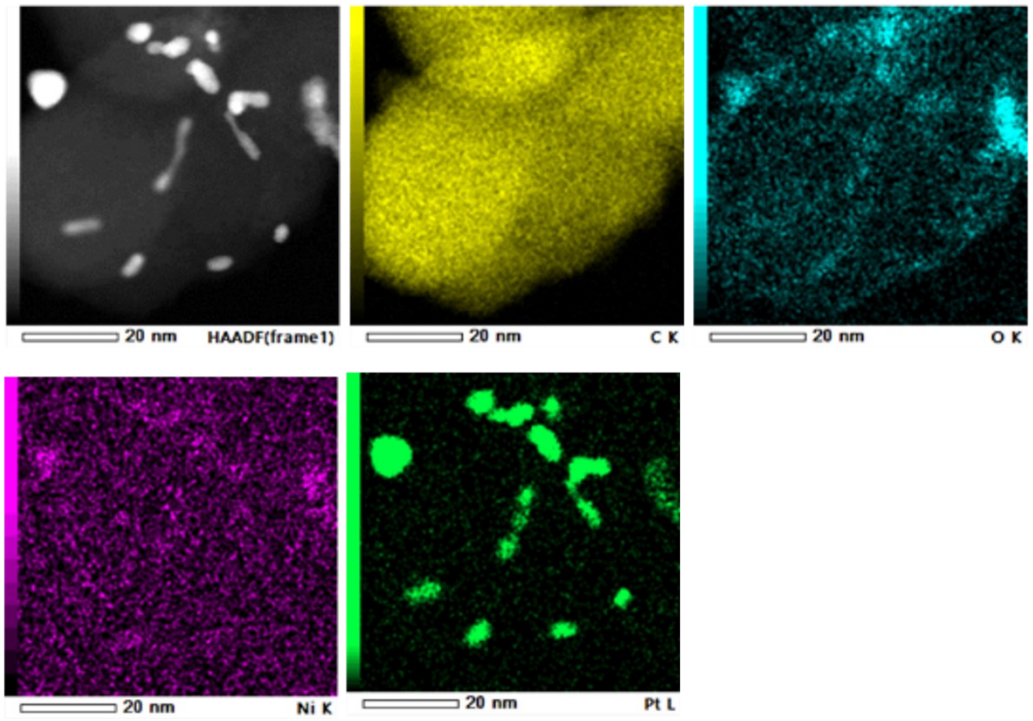

Fig. S21. STEM image and EDS element mapping for unannealed PtNi-NW/C catalyst after 10K ADT cycles.

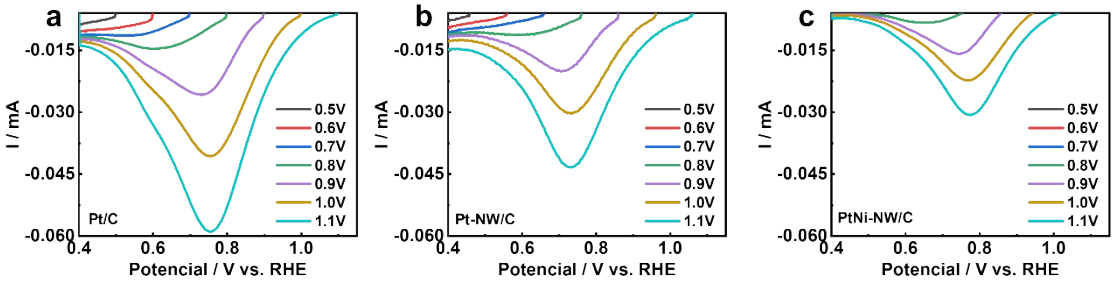

Fig. S22. Reduction current profiles of oxide species on (a) Pt/C and (b) Pt-NW/C and (c) PtNi-NW/C from 0.50 to 1.0 V *vs.* RHE.

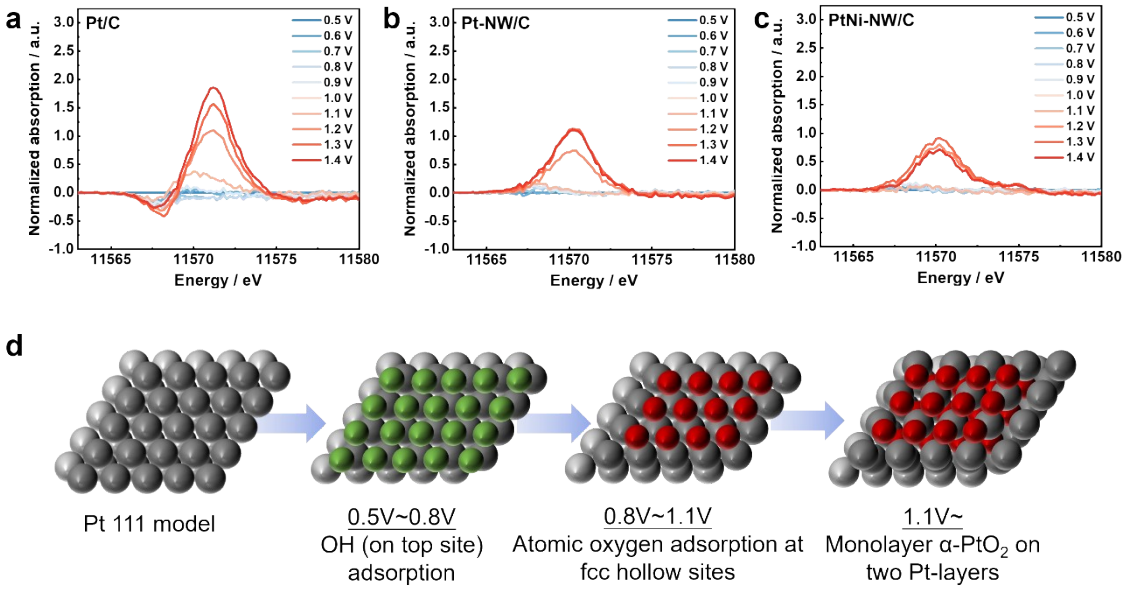

Fig. S23. (a, b, c) The difference spectra of **Fig. 5** at various potentials, the spectrum tested at 0.5 V was used as a reference spectrum. (d) The catalyst oxidation process reported by Imai et al.[1]

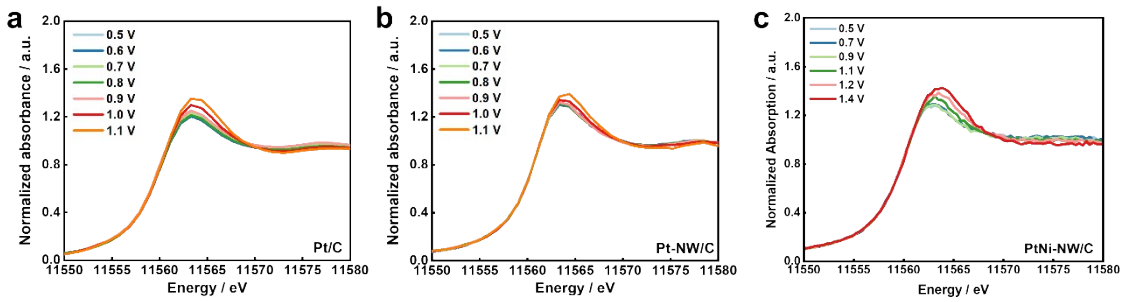

Fig. S24. Pt L_3-edge XANES spectra of (a) Pt/C, (b) Pt-NW/C and (c) PtNi-NW/C.

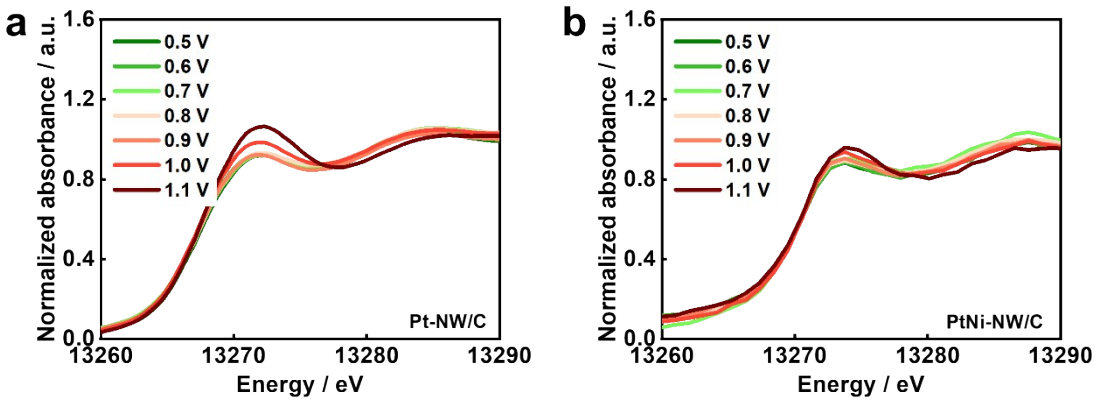

Fig. S25. Pt L_2-edge XANES spectra of (a) Pt-NW/C, (b) PtNi-NW/C.

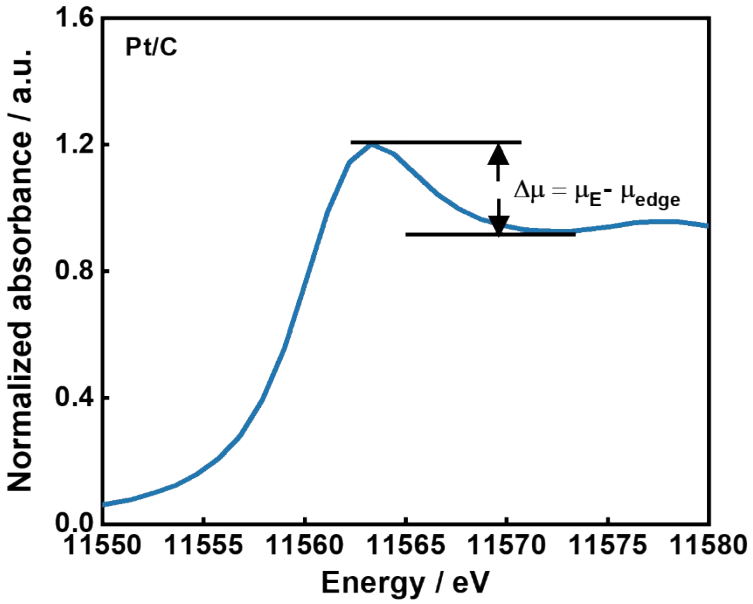

Fig. S26. XANES spectra showing the determination of the intensity on white line (Δμ) for Pt/C.

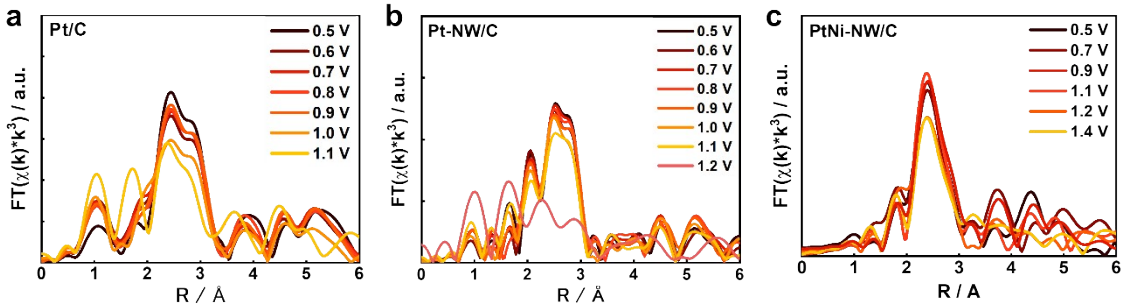

Fig. S27. The FT-EXAFS spectra for (a) Pt/C, (b) Pt-NW/C and (c) PtNi-NW/C.

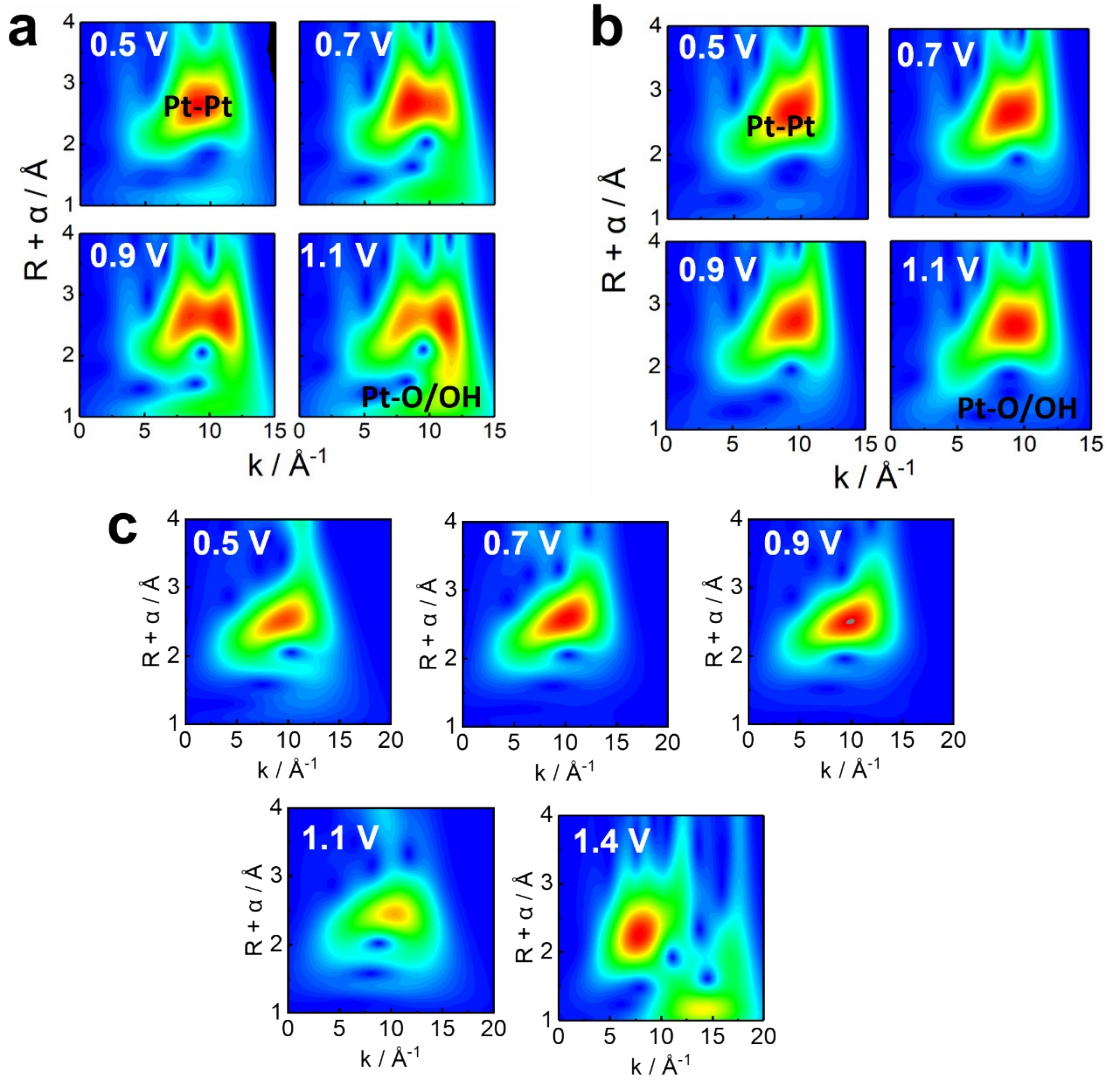

Fig. S28. WT for (a) Pt/C, (b) Pt-NW/C and (c) PtNi-NW/C at different potential.

Table S1. Fitting model and the extracted parameters of Pt nanowire

Lattice constants in / Å	XRD main	XRD sub	PDF main	PDF sub
Pt -NW/C	3.91834(13)	4.109(3)	3.92152(19)	none

Pt FCC

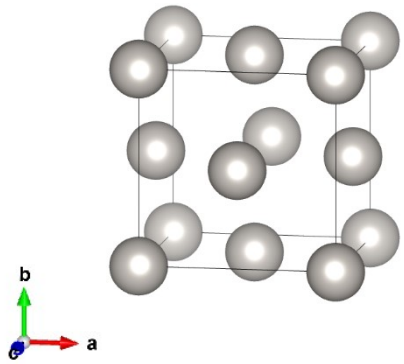

Note:

We need this additional fcc phase just to improve curve fitting. Because the nanowires exhibit anisotropic peak shapes, the expanded lattice obtained from the fitting may be imaginary.

Samples were sealed in Cole-Parmer polyimide capillaries (inner diameter: 1.0 mm). Intensity values from blank capillary measurements were subtracted from the sample data. Polarization, oblique incidence, and area corrections were applied, and the data were converted into 1D total scattering using the PIXIA program, excluding the direct beam stop region. Scattering from carbon supports was assumed to be negligible, and total scattering data from the metal nanoparticles were obtained by subtracting the Vulcan XC carbon pattern from the overall catalyst sample.

Table S2. XPS analysis result of PtNi-NW/C and Pt-NW/C.

PtNi-NW/C	**C1s**	**O1s**	**Pt4f**	**Ni2p**
Mole ratio (Normalize to C)	1.00	0.02	0.004	0.01
Elemental content ratio (mole%)	96.7	1.6	0.4	1.3
Binding Energy / eV	284.6	532.2	$4f_{7/2}$ 71.5	$2p_{3/2}$ 852.9
Pt-NW/C	**C1s**	**O1s**	**Pt4f**	
Mole ratio (Normalize to C)	1.00	0.02	0.01	
Elemental content ratio (mole%)	96.7	1.6	1.8	
Binding Energy / eV	284.6	532.2	$4f_{7/2}$ 71.5	

Table S3. Fitting model and the extracted parameters of PtNi nanowire

	BCT	Pt FCC	Ni FCC
a axis / Å	2.62603	3.78991	3.55550
C axis / Å	3.61090	-	-
Component wt%	12.96	74.58	12.45
Pt-Pt / Å	2.62603	2.67987	-

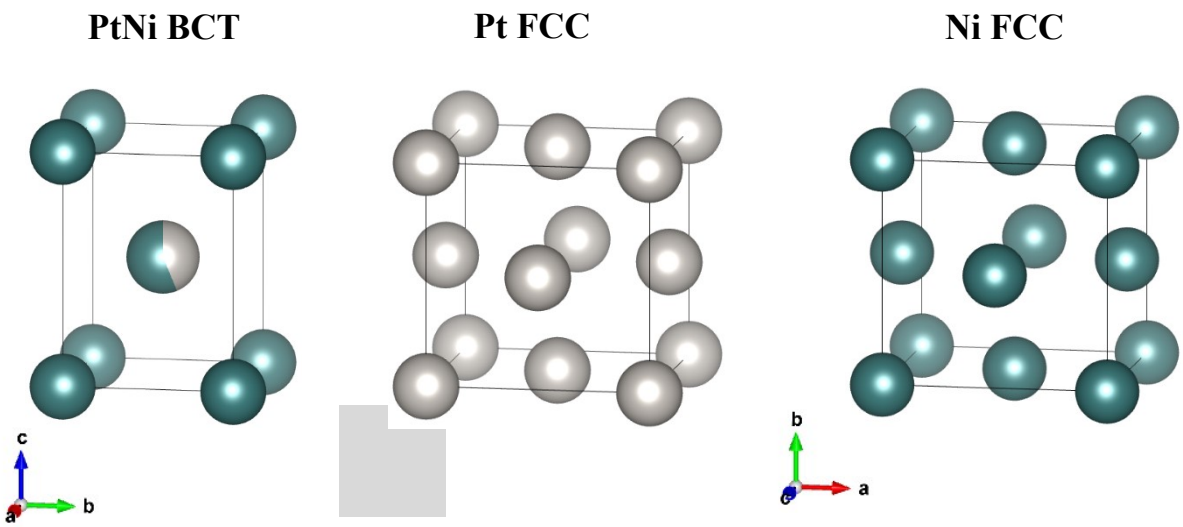

Table S4. ORR activity of PtNi-NW/C with different Ni content.

	Specific activity (mA cm^{-2})		Mass activity (A g^{-1})	
Temperature	**$Pt_{40}Ni_{60}$**	**$Pt_{25}Ni_{75}$**	**$Pt_{40}Ni_{60}$**	**$Pt_{25}Ni_{75}$**
No treat	850	928	515	529
250℃	1264	1375	709	821
400℃	1811	2074	1050	1366

Mass Activity (MA): The MA values were calculated based on the kinetic current (i_k) obtained at 0.9 V vs. RHE from the Koutecky-Levich limiting current equation. The kinetic current was normalized to the mass of Pt loaded on the electrode.

$$\frac{1}{i} = \frac{1}{i_k} + \frac{1}{i_d}$$

Specific Activity (SA): The SA values were determined by normalizing the kinetic current to the electrochemical surface area (ECSA) of the catalysts, which was calculated from the hydrogen underpotential deposition (HUPD) region in the cyclic voltammograms. The ECSA was calculated using the formula:

$$ECSA = \frac{Q_{Hupd}}{0.21\ mC\ cm^{-2}}$$

where Q_{Hupd} is the charge obtained by integrating the hydrogen adsorption peak in the cyclic voltammogram, and 0.21 mC cm^{-2} is the charge required to oxidize a monolayer of hydrogen on Pt.

Table S5. The corresponding R space curve fitting results of Pt L_3-edge for the Pt/C catalysts varying different potential. Fitting details: S_0^2 was fixed at 0.90, which was obtained by fitting the reference foils. Fits were undergone in R-space for 1.5≤R≤3.3 Å, and the k1,2,3 weighting for Δk = 3 – 11 $Å^{-1}$. The path of the Pt-Pt is from the crystal structure of FCC Pt phase (*fm-3m*).

	Bond	Length/Å	CN	ΔE/eV	Debye−Waller factor	R-factor
0.5 V	Pt-Pt	2.751(2)	9.0(2)	9.516	0.005	1.3%
0.6 V	Pt-Pt	2.750(8)	9.9(2)	10.08	0.007	1.8%
0.7 V	Pt-Pt	2.752(5)	9.5(6)	9.221	0.007	1.1%
0.8 V	Pt-Pt	2.749(9)	8.1(6)	11.50	0.005	0.7%
	Pt-O	2.109(2)	1.0(5)	1.098	0.001	
0.9 V	Pt-Pt	2.757(5)	8.0(3)	10.66	0.005	1.9%
	Pt-O	2.110(4)	1.5(5)	7.088	0.008	
1.0 V	Pt-Pt	2.763(11)	8.2(8)	10.22	0.007	2.3%
	Pt-O	2.109(3)	1.6(9)	9.925	0.008	
1.1 V	Pt-Pt	2.825(13)	5.1(9)	14.88	0.004	2.0%
	Pt-O	2.122(5)	4.1(3)	10.40	0.012	

Table S6. The corresponding R space curve fitting results of Pt L_3-edge for the Pt-NW/C catalysts varying different potential.

	Bond	Length/Å	CN	ΔE/eV	Debye−Waller factor	R-factor
0.5 V	Pt-Pt	2.746(3)	9.1(1)	8.794	0.008	0.2%
0.6 V	Pt-Pt	2.748(5)	8.9(2)	9.357	0.007	0.7%
0.7 V	Pt-Pt	2.746(5)	9.0(6)	11.32	0.006	1.5%
0.8 V	Pt-Pt	2.749(9)	9.0(5)	8.886	0.007	2.0%
0.9 V	Pt-Pt	2.752(9)	8.8(9)	10.42	0.007	0.9%
	Pt-O	2.110(4)	0.9(5)	-8.333	0.011	
1.0 V	Pt-Pt	2.748(9)	8.2(5)	-3.547	0.008	1.9%
	Pt-O	2.109(3)	1.1(5)	9.942	0.007	
1.1 V	Pt-Pt	2.779(7)	8.0(8)	7.905	0.009	2.3%
	Pt-O	2.150(4)	1.6(9)	18.85	0.005	
1.2 V	Pt-Pt	2.875(12)	3.5(9)	3.345	0.002	2.1%
	Pt-O	2.159(4)	5.1(3)	2.811	0.025	

Table S7. The corresponding R space curve fitting results of Pt L_3-edge for the PtNi-NW/C catalysts varying different potential. The corresponding R space curve fitting results of Pt L_3-edge for the Pt/C catalysts varying different potential. Fitting details: S_0^2 was fixed at 0.90, which was obtained by fitting the reference foils. Fits were undergone in R-space for 1.5≤R≤3.3 Å, and the k1,2,3 weighting for Δk = 3 – 11 $Å^{-1}$. The path of the Pt-Pt and Pt-Ni are from the crystal structure of BCT PtNi phase (*P4-mmm*) for core structure and FCC Pt phase (*fm-3m*) for Pt layer.

	Bond	Length/Å	CN	ΔE/eV	Debye−Waller factor	R-factor
0.5 V	Pt-Pt	2.677(8)	3.3(7)	2.421	0.001	0.2%
	Pt-Ni	2.639(9)	6.5(3)	7.235	0.011	
0.7 V	Pt-Pt	2.676(6)	3.3(2)	-2.419	0.008	2.0%
	Pt-Ni	2.620(9)	6.3(5)	2.149	0.011	
0.9 V	Pt-Pt	2.679(2)	3.5(5)	2.752	0.004	0.3%
	Pt-Ni	2.640(13)	6.0(5)	7.572	0.013	
1.1 V	Pt-Pt	2.682(10)	3.1(3)	5.647	0.001	1.4%
	Pt-Ni	2.651(11)	5.7(2)	5.816	0.012	
	Pt-O	2.110(4)	0.1(3)	-9.320	0.017	
1.2 V	Pt-Pt	2.686(7)	2.7(8)	-0.377	0.007	1.9%
	Pt-Ni	2.642(3)	3.5(3)	12.02	0.002	
	Pt-O	2.150(4)	1.6(3)	25.31	0.004	
1.4 V	Pt-Pt	2.711(12)	1.7(9)	17.56	0.002	
	Pt-Ni	2.647(9)	2.5(7)	6.513	0.011	0.9%
	Pt-O	2.141(4)	2.0(3)	23.96	0.012	

Table S8: Acidic ORR activity and durability of PtNi-NW/C and state-of-the-art Pt-based nanocatalysts from recent years-published work.

Catalysts	Mass activity at 0.9 V (A mg_{Pt}^{-1})	Specific activity at 0.9 V (mA cm_{Pt}^{-2})	Degradation of mass activity after ADT test		References
			Loss (%)	Cycles	
IMC-PtFeMo/C nanowire	2.56	5.41	11	10k	*Nano Energy*, 2024, **129**, 110079
PtNi/C nanowire	0.28	0.25	0	10k	*ACS Catal.,* 2024, **14**, 1750–1758
PtNi NW/C	1.85	1.64	23.6	10k	*Chin. Chem. Lett.,* 2024, **35**, 108445
PtNiGa NW/C	2.37	1.89	12.8	10k	
Pt2Ni1/C nanowire	0.095	0.24	18.9	3k	*Int. J. Hydrogen Energy.,* 2024, **51**, 1487
$L1_2$-Pt_3Co/C nanowire	0.31	2.47	6.2	5k	*Adv. Funct. Mater.,* 2024, **34**, 2311618.
A1-Pt_3Co/C nanowire	0.12	1.1	8.3	5k	
O-PtCu/C nanowire	0.48	0.47	4.2	10k	*Nano Res.*, 2024, **17**, 7001
Waved Pt nanowire/C	0.71	1.55	Na	Na	*Appl. Catal. B: Environ.*, 2023, **324**, 122268
Regular Pt nanowire/C	0.56	0.99	Na	Na	
Pt@Pt-skin Pt_3Ni nanowire	6.69	8.42	2.9	50k	*Nat. Commun.*, 2023, **14**, 1518
Pt–Ni Nanochains	1.78	3.11	35.9	10k	*Adv. Mater.*, 2023, **35**, 2206508
Pt–Ni Nanowires	1.25	2.92	58.7	10k	
Pt-Ni Bunched-Nanocages	1.95	3.55	17.4	20k	*Adv. Energy Mater.* 2023, **13**, 2204257.

PtNiCo branched nanocages	1.03	2.75	13	5k	*J. Mater. Chem. A*, 2021,**9**, 23444
PtNi branched nanocages	0.37	1.39	NA	NA	
Pt -Co nanoframes/C	0.4	0.8	15.0	10k	*Nano Lett.,* 2020, **20**, 1974
fct -PtFeIr nanowires/C	2.03	2.40	11.1	10k	*Angew. Chem.* 2022, **134**, e202113278
fcc -PtFeIr nanowires/C	1.11	1.29	31.6	10k	
$Pt_{4.31}Ga$ nanowires/C	1.89	3.28	15.8	30k	*J. Am. Chem. Soc.* 2019, **141**, 18083
Jagged Pt nanowires/C	13.6	11.5	12	6k	*Science*, 2016, **354**,1414
Pt_3Ni nanowires/C	0.546	0.9	63	50k	*ACS Catal.*, 2019, **9**, 4488
$L1_0$-PtCo/C NW	1.30	3.55	NA	10k	*ACS Appl. Mater. Interfaces*, 2022, **14**, 25246
Re-PtNiGa tetrametallic NWs/C	3.49	3.17	10.6	20k	*Appl. Catal. B: Environ.*, 2022, **303**, 120918
PtNi NWs/C	2.11	2.40	48.9	20k	
$WO_{x-(0.25)}$-PtNi NWs/C	0.85	1.29	23.89	30k	*J. Colloid Interface Sci.*, 2022, **607**, 1928
PtNi NWs/C	0.33	0.60	45.94	30k	
$Pt/W_{0.02}–SnO_2–C$	0.23	0.37	10.0	50k	*J. Mater. Chem. A*, 2024,**12**,10799
$L1_2$-$PtCu_3$/C	1.33	2.63	27.1	20k	*J. Mater. Chem. A*, 2024,**12**,10385
PtZn–CoNC	0.45	0.55	12.8	30k	*J. Mater. Chem. A*, 2023,**11**, 24371
PtNi-NW/C	**1.37**	**2.07**	**5.1**	**10k**	**This work**

Reference

1. H. Imai, K. Izumi, M. Matsumoto, Y. Kubo, K. Kato and Y. Imai, *J. Am. Chem. Soc.*, 2009, **131**, 6293-6300.